



Published in final edited form as:

Am J Obstet Gynecol. 2013 September ; 209(3): 227.e1–227.e11. doi:10.1016/j.ajog.2013.04.036.

Maternal Engineered Nanomaterial Exposure and Fetal Microvascular Function: Does the Barker Hypothesis Apply?

Phoebe A. STAPLETON, PhD,

Morgantown, WV; Center for Cardiovascular and Respiratory Sciences and Department of Physiology and Pharmacology, West Virginia University School of Medicine

Ms. Valerie C. MINARCHICK, BS,

Morgantown, WV; Center for Cardiovascular and Respiratory Sciences and Department of Physiology and Pharmacology, West Virginia University School of Medicine

Jinghai YI, PhD,

Morgantown, WV; Center for Cardiovascular and Respiratory Sciences and Department of Physiology and Pharmacology, West Virginia University School of Medicine

Mr. Kevin ENGELS, BS,

Morgantown, WV; Center for Cardiovascular and Respiratory Sciences and Department of Physiology and Pharmacology, West Virginia University School of Medicine

Mr. Carroll R. McBRIDE, BS, and

Morgantown, WV; Center for Cardiovascular and Respiratory Sciences and Department of Physiology and Pharmacology, West Virginia University School of Medicine

Timothy R. NURKIEWICZ, PhD

Morgantown, WV; Center for Cardiovascular and Respiratory Sciences, Department of Physiology and Pharmacology and Department of Neurobiology and Anatomy, West Virginia University School of Medicine

Abstract

Objective—The continued development and use of engineered nanomaterials (ENM) has given rise to concerns over the potential for human health effects. While the understanding of cardiovascular ENM toxicity is improving, one of the most complex and acutely demanding “special” circulations is the enhanced maternal system to support fetal development. The “Barker Hypothesis” proposes that fetal development within a hostile gestational environment may predispose/program future sensitivity. Therefore, the objective of this study was two-fold: 1) to determine if maternal ENM exposure alters uterine and/or fetal microvascular function and 2) test the Barker Hypothesis at the microvascular level.

© 2013 Mosby, Inc. All rights reserved.

Address For Reprints and Correspondence: Timothy R. Nurkiewicz, Ph.D. Center for Cardiovascular and Respiratory Sciences 1 Medical Center Drive Robert C. Byrd Health Sciences Center West Virginia University Morgantown, WV, 26506-9105 office: (304) 293-7328 fax: (304) 293-5513 tnurkiewicz@hsc.wvu.edu.

Publisher's Disclaimer: This is a PDF file of an unedited manuscript that has been accepted for publication. As a service to our customers we are providing this early version of the manuscript. The manuscript will undergo copyediting, typesetting, and review of the resulting proof before it is published in its final citable form. Please note that during the production process errors may be discovered which could affect the content, and all legal disclaimers that apply to the journal pertain.

The author(s) report(s) no conflict of interest.

An abstract has been accepted to present this work at the 52nd Annual Meeting of the Society of Toxicology, San Antonio TX, to be held March 10-14, 2013.

Study Design—Pregnant (gestation day 10) Sprague-Dawley rats were exposed to nano-titanium dioxide aerosols (11.3 ± 0.039 (mg/m³)*hour, 5 hours/day, 8.2 ± 0.85 days) to evaluate the maternal and fetal microvascular consequences of maternal exposure. Microvascular tissue isolation (gestation day 20) and arteriolar reactivity studies (<150 μ m passive diameter) of the uterine premyometrial and fetal tail arteries were conducted.

Results—ENM exposures led to significant maternal and fetal microvascular dysfunction which presented as robustly compromised endothelium-dependent and -independent reactivity to pharmacologic and mechanical stimuli. Isolated maternal uterine arteriolar reactivity was consistent with a metabolically impaired profile and hostile gestational environment, impacting fetal weight. The fetal microvessels isolated from exposed dams demonstrate significant impairments to signals of vasodilation specific to mechanistic signaling and shear stress.

Conclusion—To our knowledge, this is the first report providing evidence that maternal ENM inhalation is capable of influencing fetal health, thereby supporting that the Barker Hypothesis is applicable at the microvascular level.

Keywords

Microvascular; Barker Hypothesis; Engineered Nanomaterials (ENM)

INTRODUCTION

Anthropogenic engineered nanomaterials (ENM) are specifically manufactured for their unique properties at the nanometer scale (<100 nm in one dimension).^{1,2} While their applicability may appear infinite, significant resources have been committed to focus ENM development on engineering and biomedical applications.³ ENM have already impacted public health through diverse daily uses (e.g. surface coatings, cosmetics, food, drug delivery systems, and implantable medical devices). In many of these applications adult toxicities have been observed; however, the fetal consequences of maternal exposure to ENM are essentially unknown.

Fetal toxicity and the genetic basis of adult disease is an initiative within the National Institute of Environmental Health and Safety (NIEHS).⁴ The general understanding of adult cardiovascular ENM toxicity is modest to good⁵; yet, the maternal and fetal consequences of maternal ENM exposures during gestation are unknown. The “Barker Hypothesis” proposes that the association between retarded growth and cardiovascular disease is due to chronic physiologic and metabolic effects imposed upon a fetus by a hostile gestational environment.^{6,7} Limited animal and *in vitro* studies suggest that maternal ENM exposure has direct consequences on the uterus, placenta, and fetus.⁸⁻¹⁰ Injected ENM have been shown to easily reach the uterus and stimulate uterine atrophy.¹¹ Similarly, intravenous maternal ENM exposure also compromises gestation by causing placental vascular lesions and stimulating ROS production.⁸ The most striking observations are structural and functional fetal abnormalities after maternal ENM exposure: impaired implanted fetal resorption (principally in the late gestation), reduction in the number of live fetuses delivered¹², impaired postnatal growth and weight gain^{8,10} and generalized neurophysical deficits or neurobehavioral alterations in their offspring.^{11,13,14} While these proof-of-principle studies have shed light on an extremely important issue, injecting high ENM doses to produce significant repeatable results. Furthermore, these studies have not focused on the most likely route of ENM exposure, inhalation. Lastly, the functional microvascular ramifications from the maternal or fetal perspective have never been studied in these regards.

The microcirculation is the principal level of the vasculature for a host of physiological parameters including: growth, metabolism, peripheral resistance, tissue perfusion, nutrient/waste exchange, permeability, and leukocyte trafficking. Virtually every pathologic development has a microvascular origin and/or consequence. Our research program has advanced a generally good understanding of the systemic consequences of inhaled ENM in the coronary and skeletal muscle microcirculations^{5;15;16}; however, no work has been done in regards to pregnancy. For example, it has only recently been shown that environmental particulate matter (PM; air pollution) inhalation is associated with maternal blood pressure disturbances and low birth weights.¹⁷⁻¹⁹ ENM differ significantly from PM due to their homozygous composition, unique properties associated with their small size, and potential toxicities associated with intentional exposures.

Functionally, the microcirculation acts to regulate blood flow distribution while protecting downstream tissues from high arterial pressures and flow rates, roles which are crucial for fetal health and survival of a pregnancy. Precise maintenance of blood flow, within an environment of profound remodeling and growth, is paramount for maternal health and fetal development. ENM exposure has been shown to impair normal microvascular reactivity and function²⁰ in a range of vascular beds, including heart^{15;16} and skeletal muscle.^{21;22} It is reasonable to speculate that maternal ENM exposure may also influence normal uterine function, leading to a hostile gestational environment, which is capable of impairing fetal microvascular reactivity. Therefore, the purpose of this study was to test the Barker Hypothesis from a microvascular prospective.

MATERIALS AND METHODS

Animal Model

Sprague Dawley rats (250-275g female; 300-325g male) were purchased from Hilltop Laboratories (Scottsdale, PA). Rats were housed at West Virginia University with food and water provided *ad libitum* and acclimated for at least 72-hours before use or mating. Females were monitored prior to breeding to ensure estrus, at which time each female was placed with an individual male. Female rats were then smeared every 12-hours to verify breeding via the presence of sperm. To ensure that all methods were performed humanely and with regard to alleviation of suffering, all procedures were approved by the Institutional Animal Care and Use Committee of the West Virginia University.

ENM

Nano-titanium dioxide (TiO₂) powder was obtained from Evonik (Aeroxide TiO₂, Parsippany, NJ). This ENM is a mixture composed of anatase (80%) and rutile (20%) TiO₂, with a primary particle size of 21 nm, and a surface area of 48.08 m²/g.²²⁻²⁴ The nano-TiO₂ was prepared for aerosolization by drying, sieving, and storing the powder.^{21;22}

Inhalation Exposure

We have previously reported and described the nano-aerosol generator and exposure system used for the current experiments (U.S. Patent #13/317,472).^{21;22;25;26} Briefly, the system was developed specifically for rodent particle inhalation exposures. The apparatus was developed with a vibrating fluidized bed, a Venturi vacuum pump, cyclone separator, impactor and mixing device, an animal housing chamber, and real-time monitoring devices with feedback control. Aerosols were generated by allowing a high velocity air stream to pass through the vibrating fluidized bed and into the Venturi vacuum pump; drawing air and the nano-TiO₂ as it passes. Aerosols enter the cyclone separator, which is gated to removed agglomerates >400 nm at an input flow rate of 60 l/min of clean dry air before entering the exposure chamber.

Size distribution, mean aerodynamic diameter, and relative mass concentration of the aerosols were monitored in real time (Electrical Low Pressure Impactor (ELPI), Dekati, Tempere, Finland) while the particle size distribution was also measured in real-time with a Scanning Mobility Particle Sizer device (SMPS; TSI Inc., St. Paul, MN). Once the steady-state aerosol concentration was achieved, exposure duration was adjusted to achieve a daily calculated deposition of $45 \pm 2 \mu\text{g}$. Animals were exposed for 5 hours per day for an average of 8.2 ± 0.85 days at a final mass concentration of 11 mg/m^3 or to filtered air (0 mg/m^3 , control). Calculated total deposition was calculated based on mouse methodology previously described and normalized to rat weight and to pregnant rat minute ventilation^{15;27;28} using the equation: $D = F * V * C * T$, where F is the deposition fraction (10%), V is the minute ventilation based on body weight, C equals the mass concentration (mg/m^3), and T equals the exposure duration (minutes).²²

Tissue Preparation

Pregnant rats were anesthetized with isoflurane (5% induction, 2% maintenance) on day 20, 24-hours after the last exposure.^{15;16;29} Rats were euthanized by exsanguination, after which the uterus was removed, flushed of excess blood, and placed in a dish of chilled (4°C) physiological salt solution (PSS). The uterus was visually inspected for evidence of partial resorption, while fetal tissue was removed and weighed.

Microvessel Isolation

Maternal—Despite their label, premyometrial radial uterine arteries are considered representative of the uterine microcirculation based on passive diameter ($\sim 150 \mu\text{m}$)³⁰, anatomic position within the parenchyma, representing the 3rd to 4th order branching pattern, and functional vascular resistance (systemic pressure decreases of approximately 100 mmHg ³¹). The uterus was pinned to visualize the vasculature and a distal segment of the radial artery was isolated, removed, transferred to a vessel chamber (Living Systems Instrumentation, Burlington, VT) containing fresh oxygenated PSS, cannulated with glass pipettes, and secured using nylon suture (11-0 ophthalmic, Alcon, U.K.). Arterioles were extended to their *in situ* length, pressurized to 60 mmHg with physiological salt solution (PSS), superfused with warmed (37°C) oxygenated (21% O_2 -5% CO_2 -74% N_2) PSS at a rate of 10 mL/min , and allowed to develop spontaneous tone.^{16;30;32} Internal and external arteriolar diameters were measured digitally with video calipers (Colorado Video, Boulder, CO) and recorded.

Fetal—Pups were pinned supine within a chilled (4°C) dissecting chamber filled with PSS. The tail artery was isolated, excised, and transferred to the vessel chamber described above. The tail artery was selected for study because: (1) it is primarily responsible for thermal homeostasis and is fully functional at birth,³³ (2) provides a significant pressure gradient from the proximal to the distal end of the tail, creating resistance, a representative characteristic of the microcirculation,³⁴ and (3) other vascular beds within the pup were considered too short to successfully cannulate, due to the excessive branching associated with tissue growth and development. To maintain consistency between experiments, fetal arteries were pressurized to 60 mmHg .

Arteriolar Reactivity

Following equilibration, arteriolar reactivity was evaluated in random order to ensure responses were neither interactive nor time-dependent over the course of the experiment in response to: 1) luminal flow changes to elicit a shear stress response (reductions and increases in flow from 0 $\mu\text{L/min}$ to 30 $\mu\text{L/min}$ at 5 $\mu\text{L/min}$ increments); 2) acetylcholine (ACh) (10^{-9} – 10^{-4} M); 3) spermine NONOate (SPR) (10^{-9} – 10^{-4} M); and 4) phenylephrine

(PE) (10^{-9} – 10^{-4} M). Following assessments of arteriolar reactivity, the superfusate was replaced with Ca^{2+} -free PSS until passive tone could be established (<150 μm maximum diameter).

Statistics and Formulae

Data are expressed as means \pm SE. Spontaneous tone was calculated by the equation: $[(D_M - D_I)/D_M] * 100$, where D_M is the maximal diameter recorded at 60 mmHg under Ca^{2+} -free PSS as described above, and D_I is the initial steady-state diameter achieved prior to experimental period. Vessels were used for experiments only if spontaneous tone $\geq 20\%$ was achieved.

The experimental responses to ACh, SPR, and PE are presented as percent relaxation from baseline diameter: $[(D_{SS} - D_{CON})/(D_M - D_{CON})] * 100$, where D_{SS} remains the steady-state diameter achieved after each chemical bolus, and D_{CON} is the control diameter measured immediately prior to the dose-response experiment. All experimental periods were at least 2 minutes, and all steady-state diameters were collected for at least one minute. Representing the responses in this manner allowed us to normalize for potential differences in baseline diameters before each dose-response curve.

Shear stress was calculated from volumetric flow (Q) according to the equation: $\tau = 4\eta Q / \pi r^3$, where η represents viscosity (0.8 centipoise, (cP)), Q represents volumetric flow rate (measured with a calibrated flow indicator, Living Systems Instrumentation, Burlington, VT), and r equals the vessel radius.

Student's t-tests were used to compare sham and exposed animal and vessel characteristics. The t-test was also used to evaluate differences between animals exposed for ≤ 7 days with those exposed for >7 days. Concentration-diameter (ACh, PE, and SPR) and flow-diameter curves were assessed by two-way repeated measures ANOVA to detect differences between and within groups. Pairwise comparisons post-hoc analysis comparisons (Bonferroni) were made if significance ($P \leq 0.05$) was reached (SigmaPlot 11.0, Systat Software Inc., San Jose, CA). Equations of 1st-order regression lines were developed to assess line slope relationships (GraphPad Software, Prism).

RESULTS

ENM exposure and uterine health

There were expected significant differences between the pregnant sham and exposed rats with respect to days of exposure, concentration, calculated total exposure, and calculated total deposition by experimental design (Table 1). These differences did not affect litter size, litter weight, or the average pup weight. However, when the exposed rats were broken down based on days of exposure, there was a significant difference in litter weight (Table 1). These results indicate a longer duration of exposure during gestation, greater exposure concentration, or exposure earlier in a pregnancy has a greater impact on fetal development.

Overall, shorter exposures (<7 days) were favored to increase experimental success, because with longer exposures (>7 days) whole litters were lost to fetal death or varying stages of fetal resorption. Therefore, for the remainder of the studies, analysis will remain exposed versus sham groups.

Microvascular characteristics

There were no significant differences between the pregnant rats with respect to age, weight, or passive uterine radial artery diameter (Table 2A). However, there were significant

differences between sham and exposed uterine radial artery active diameter and spontaneous vessel tone prior to interventions. These results provide evidence that indicate ENM exposure leads to increased uterine vascular tone and smaller active diameter. If this were to persist *in vivo*, this increase in peripheral resistance may reduce uterine blood flow or alter the distribution of blood flow within or between uterine horns due to bidirectional flow. Unlike humans, within a rodent model of pregnancy, the arcading network of blood flow supplies a constant perfusion within the uterus allowing for multiple pup litters³⁵

With respect to the fetal tail arteries, there were no significant differences in age, spontaneous active diameter, passive diameter, or vascular tone (Table 2B). Unintentionally, the fetal tissue studied from exposed dams was significantly larger than the sham group (Table 2B).

Aerosolized ENM distribution

Figure 1 is a graphical representation of the nanoparticle diameter distribution. The primary diameter of nano-TiO₂ is 21 nm; however these particles tend to agglomerate, leading to an aerodynamic diameter of 149 nm ± 3.9, consistent with other experiments within our research program^{21, 25}. Therefore, when aerosolized it is important to monitor particle characteristics in real-time to maintain a consistent aerosol distribution within and between experiments.

Endothelium-Dependent Vasodilation

Maternal endothelium-dependent arteriolar dilation is significantly attenuated after ENM exposure (Figure 2A). Reduced endothelium-dependent dilation through ACh stimulation may be attributed to an alteration to NO signaling; however, ACh also leads to signaling through pathways of arachidonic acid metabolism (prostacyclin, lipoxygenase). Therefore, while NO signaling may be significantly perturbed, residual endothelium-dependent dilation may be due to alternate signaling pathways.

Fetal endothelium-dependent reactivity of fetal vessels after maternal exposure was abolished compared to control (Figure 2B). This impairment may also be due to a decrease in NO bioavailability, decreased NO production, inhibition of soluble guanylyl cyclase (sGC), or an increase in oxidative NO scavenging, in combination with a shift in arachidonic acid-cyclooxygenase signaling toward thromboxane A₂ generation. Overall, ENM exposure during pregnancy significantly alters fetal endothelium-dependent dilation.

Endothelium-Independent Vasodilation

Uterine endothelium-independent dilation was also blunted after nanomaterial exposure (Figure 3A). This impairment indicates smooth muscle NO sensitivity is altered and may account for the smaller active diameter and increased vessel tone (Table 2A). Perhaps the most striking result is that endothelium-independent reactivity was abolished in the fetal vasculature (Figure 3B). This lack of NO reactivity in conjunction with the endothelium-dependent impairments highlighted in Figure 2 indicates a tremendous compromise of normal microvascular dilation within the fetal vasculature. In adulthood, this dysfunction may predispose those exposed to ENM during gestation to cardiovascular disease (i.e. hypertension or peripheral vascular disease).

Smooth Muscle Contractility

PE was used to evaluate vascular smooth muscle α -adrenergic sensitivity. Uterine smooth muscle sensitivity to α -adrenergic stimulation is augmented after nanomaterial exposure (Figure 4A). This sensitivity was not altered in fetal tail arteries (Figure 4B), indicating a

propensity toward increased tone and vasodilation in uterine arterioles, and leading to an overall reduction in tissue perfusion.

Active Mechanotransduction

Uterine arterioles from pregnant ENM exposed rats, display a reduced dilation in response to increases in intraluminal flow rate (10-30 $\mu\text{L}/\text{min}$) (Figure 5A). The vascular endothelium is exposed to a large variation in shear stress that is fundamentally a function of vessel radius; therefore shear stress was plotted against increases in volumetric flow (Figure 5B). These data provide evidence that shear stress increased with intraluminal flow. In ENM exposed rats uterine vessels inappropriately constrict in response to increasing intraluminal flow. This causes significant increases in shear stress compared to the control. A failure of the vasculature to dilate in this capacity results in elevated shear forces exerted on the vascular wall. In Figure 5C, evidence of this is provided where uterine radial artery dilation is presented as a function of shear stress.

Similarly, progeny of exposed dams displayed a reduced vasodilation in response to increasing intraluminal flow (5-30 $\mu\text{L}/\text{min}$) (Figure 6A). The linear relationship between calculated shear stress and stepwise increases in intraluminal flow in fetal tail arteries shows positive relationships between volumetric flow and shear stress (Figure 6B). In Figure 7C, fetal tail artery vasodilation is presented as a function of shear stress.

With respect to shear stress, uterine arterioles from pregnant rats exposed to ENM and the progeny of those rats are either unable to effectively sense this stimulus, properly respond, or both. Failure to respond appropriately (or dilate) to mechanical stimuli can lead to increases in tissue damage, organ pathology, and severity of disease (i.e. hypertension).

COMMENT

We have demonstrated for the first time that: (1) maternal ENM exposure severely impairs uterine microvascular reactivity and (2) ENM exposure during pregnancy can severely impact fetal vascular reactivity.

Gestation necessitates rapid microvascular growth and functionalization to maintain a healthy pregnancy. The uterine microcirculation has a substantial NO dependence during pregnancy³⁶ through augmented response to ACh³⁷ and an increase in endothelial nitric oxide synthase regulation.³⁸ This increased NO dependence not only improve vasodilation, but also offset vasoconstrictive influences. Our results provide evidence that maternal ENM exposure impairs endothelium-dependent and endothelium-independent dilation (Figure 2A and 3A). Additionally, maternal adrenergic sensitivity is augmented (Figure 4A). These results are consistent with investigations describing enhanced myogenic tone as a result of NO impairment due to maternal nutritional status.^{39;40}

It has been theorized that different levels of the vasculature are regulated by distinctive mechanisms; specifically that small downstream arterioles are more sensitive to metabolic mediators, while larger upstream vessels are more responsive to mechanical signaling (i.e. alterations to intraluminal flow)⁴¹. In this model, signaling at the microvascular level, for example NO, would lead to dilation resulting in an upstream decrease in pressure and subsequent upstream dilation resulting in a net increase in blood flow, fulfilling metabolic demand. Failure to dilate normally to these signals results in an increase in tangential forces on the arterial wall, an inability to appropriately distribute blood flow, and an increase of tissue damage due to ischemia or localized hypertension. Taken together, Figures 2A-4A and Figure 5, provide evidence of a failure within the uterine microcirculation to respond properly to normal metabolic and mechanotransduction signals, leading to the possibility of

further endothelial cell damage, due to the significantly high shear stress. Collectively, these signaling patterns may create a hostile gestational environment for the developing offspring.

Fetal programming after maternal ENM exposure may have effects lasting well into adulthood. Tail arteries isolated from these pups displayed an impaired vasodilation that was similar to that observed in the uterine arterioles after maternal nano-TiO₂ inhalation; however, the intensity of the fetal impairments to NO stimulated dilation were significantly more severe (Figure 2A vs. 2B and 3A vs. 3B). This may indicate prenatal alterations to NO signaling mechanisms (sGC inhibition) or due to the development of differing vascular beds. It is concerning that these pups display difficulty reacting to increased shear stress, although not to significance (Figure 6C) at this young age. Early stage endothelial cell dysfunction⁴² is a hallmark of many cardiovascular diseases is, a condition rarely identified in models so young. These outcomes provide further evidence not only supporting the Barker Hypothesis from a microvascular perspective.

While it appears that ENM inhalation did not affect litter size or pup weight, it should be noted that maternal exposures from 5-13 days. In longer maternal exposures (earlier in the pregnancy) 2-4 pups/litter were very ischemic and were either poorly reabsorbed or would not have survived (images not shown). Additionally, these longer exposures led to significantly smaller litters overall, with a decreased pup number, decreased overall litter weight, and decreased average weight per pup (Table 1). Therefore, it seems likely that there may be a temporal effect of ENM exposure where early to mid-gestation exposures may result in far more dire consequences for the offspring.

To our knowledge, this is the first report that maternal ENM inhalation creates a hostile gestational environment capable of impacting fetal health. Therefore, future directions should include a more thorough investigation into the mechanisms supporting these alterations, including a comprehensive interrogation of pressure regulation, as regulation is crucial to maternal health and fetal development. Additional studies stemming from maternal ENM exposure include transcriptomic, epigenetic, and proteomic studies of the progeny, determining the temporal association of maternal exposure (timing of exposure during gestation and length of exposure) during pregnancy, and exploring the long-term consequences suffered by the progeny.

In summary, these results provide strong evidence that indicates while vascular function may appear under basal conditions when challenged to react to normal physiological stimuli, the uterine radial arteries of pregnant females exposed to ENM and the vasculature of the progeny of these dams display robust dysfunctional responses. These outcomes are consistent with the foundation of a hostile gestational environment. Taken as whole, this ENM exposure study is consistent with the Barker Hypothesis from a microvascular perspective.

Acknowledgments

The authors thank Ms. Kimberly Wix from West Virginia University Department of Physiology and Pharmacology for her expert technical assistance in this study. This work was supported by the National Institutes of Health [RO1-ES015022 (TRN) and RC1-ES018274 (TRN)], the National Science Foundation [NSF-1003907 (VCM)], and National Science Foundation, Cooperative Agreement EPS-1003907.

REFERENCES

1. Borm PJ, Muller-Schulte D. Nanoparticles in drug delivery and environmental exposure: same size, same risks? *Nanomedicine.(Lond)*. 2006; 1:235–49. [PubMed: 17716113]

2. Mossman BT, Borm PJ, Castranova V, Costa DL, Donaldson K, Kleeberger SR. Mechanisms of action of inhaled fibers, particles and nanoparticles in lung and cardiovascular diseases. *Part Fibre.Toxicol.* 2007; 4:4. [PubMed: 17537262]
3. Borm PJ, Robbins D, Haubold S, Kuhlbusch T, Fissan H, Donaldson K, et al. The potential risks of nanomaterials: a review carried out for ECETOC. *Part Fibre.Toxicol.* 2006; 3:11. [PubMed: 16907977]
4. National Institute of Environmental Health Sciences. Linking Early Environmental Exposures to Adult Diseases. NIEHS; 2012. 11-28-2012
5. Nurkiewicz TR, Porter DW, Hubbs AF, Stone S, Moseley AM, Cumpston JL, et al. Pulmonary Particulate Matter and Systemic Microvascular Dysfunction. *Res.Rep.Health Eff.Inst.* 2011
6. Barker DJ, Martyn CN. The maternal and fetal origins of cardiovascular disease. *J.Epidemiol.Community Health.* 1992; 46:8–11. [PubMed: 1573367]
7. Barker DJ. The fetal and infant origins of adult disease. *BMJ.* 1990; 301:1111. [PubMed: 2252919]
8. Pietroiusti A, Massimiani M, Fenoglio I, Colonna M, Valentini F, Palleschi G, et al. Low doses of pristine and oxidized single-wall carbon nanotubes affect mammalian embryonic development. *ACS Nano.* 2011; 5:4624–33. [PubMed: 21615177]
9. Long TC, Tajuba J, Sama P, Saleh N, Swartz C, Parker J, et al. Nanosize titanium dioxide stimulates reactive oxygen species in brain microglia and damages neurons in vitro. *Environ.Health Perspect.* 2007; 115:1631–37. [PubMed: 18007996]
10. Blum JL, Xiong JQ, Hoffman C, Zelikoff JT. Cadmium associated with inhaled cadmium oxide nanoparticles impacts fetal and neonatal development and growth. *Toxicol.Sci.* 2012; 126:478–86. [PubMed: 22240978]
11. Yamashita K, Yoshioka Y, Higashisaka K, Mimura K, Morishita Y, Nozaki M, et al. Silica and titanium dioxide nanoparticles cause pregnancy complications in mice. *Nat.Nanotechnol.* 2011; 6:321–28. [PubMed: 21460826]
12. Fujitani T, Ohyama K, Hirose A, Nishimura T, Nakae D, Ogata A. Teratogenicity of multi-wall carbon nanotube (MWCNT) in ICR mice. *J.Toxicol.Sci.* 2012; 37:81–89. [PubMed: 22293413]
13. Hougaard KS, Jackson P, Jensen KA, Sloth JJ, Loschner K, Larsen EH, et al. Effects of prenatal exposure to surface-coated nanosized titanium dioxide (UV-Titan). A study in mice. *Part Fibre.Toxicol.* 2010; 7:16. [PubMed: 20546558]
14. Ema M, Kobayashi N, Naya M, Hanai S, Nakanishi J. Reproductive and developmental toxicity studies of manufactured nanomaterials. *Reprod.Toxicol.* 2010; 30:343–52. [PubMed: 20600821]
15. Stapleton PA, Minarchick VC, Cumpston AM, McKinney W, Chen BT, Sager TM, et al. Impairment of Coronary Arteriolar Endothelium-Dependent Dilation after Multi-Walled Carbon Nanotube Inhalation: A Time-Course Study. *International Journal of Molecular Science.* 2012; 13:13781–803.
16. LeBlanc AJ, Cumpston JL, Chen BT, Frazer D, Castranova V, Nurkiewicz TR. Nanoparticle inhalation impairs endothelium-dependent vasodilation in subepicardial arterioles. *J.Toxicol.Environ.Health A.* 2009; 72:1576–84. [PubMed: 20077232]
17. Hampel R, Lepeule J, Schneider A, Bottagisi S, Charles MA, Ducimetiere P, et al. Short-term impact of ambient air pollution and air temperature on blood pressure among pregnant women. *Epidemiology.* 2011; 22:671–79. [PubMed: 21730862]
18. Jedrychowski WA, Perera FP, Maugeri U, Spengler J, Mroz E, Flak E, et al. Prohypertensive effect of gestational personal exposure to fine particulate matter. Prospective cohort study in non-smoking and non-obese pregnant women. *Cardiovasc.Toxicol.* 2012; 12:216–25. [PubMed: 22328329]
19. van den Hooven EH, Pierik FH, de KY, Willemsen SP, Hofman A, van Ratingen SW, et al. Air pollution exposure during pregnancy, ultrasound measures of fetal growth, and adverse birth outcomes: a prospective cohort study. *Environ.Health Perspect.* 2012; 120:150–56. [PubMed: 22222601]
20. Stampfl A, Maier M, Radykewicz R, Reitmeir P, Gottlicher M, Niessner R. Langendorff heart: a model system to study cardiovascular effects of engineered nanoparticles. *ACS Nano.* 2011; 5:5345–53. [PubMed: 21630684]

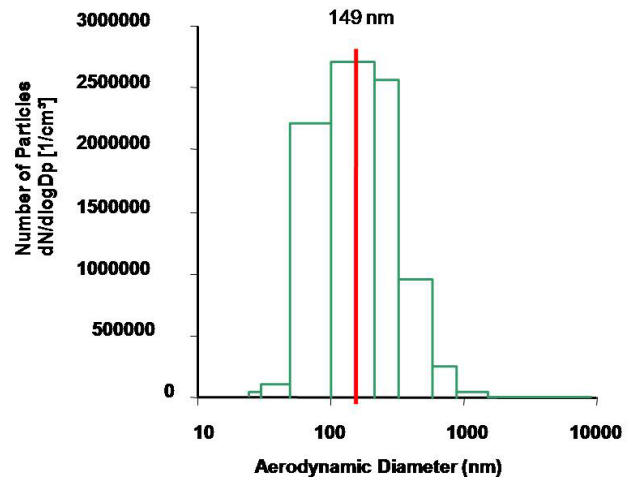
21. Knuckles TL, Yi J, Frazer DG, Leonard HD, Chen BT, Castranova V, et al. Nanoparticle inhalation alters systemic arteriolar vasoreactivity through sympathetic and cyclooxygenase-mediated pathways. *Nanotoxicology*. 2011
22. Nurkiewicz TR, Porter DW, Hubbs AF, Cumpston JL, Chen BT, Frazer DG, et al. Nanoparticle inhalation augments particle-dependent systemic microvascular dysfunction. *Part Fibre.Toxicol*. 2008; 5:1. [PubMed: 18269765]
23. Sager TM, Castranova V. Surface area of particle administered versus mass in determining the pulmonary toxicity of ultrafine and fine carbon black: comparison to ultrafine titanium dioxide. *Part Fibre.Toxicol*. 2009; 6:15. [PubMed: 19413904]
24. Sager TM, Kommineni C, Castranova V. Pulmonary response to intratracheal instillation of ultrafine versus fine titanium dioxide: role of particle surface area. *Part Fibre.Toxicol*. 2008; 5:17. [PubMed: 19046442]
25. Yi J, Chen BT, Schwegler-Berry DE, Frazer DG, Castranova V, McBride CR, Knuckles TL, Stapleton PA, Minarchick VC, Nurkiewicz TR. Whole-Body Nanoparticle Aerosol Inhalation Exposures. *Journal of Visualized Experiments* . 2013 In Production.
26. Yi, J.; Nurkiewicz, TR. Nanoparticle Aerosol Generator.. 2011. 13/317,472 U. S. Patent Application
27. Porter DW, Hubbs AF, Chen BT, McKinney W, Mercer RR, Wolfarth MG, et al. Acute pulmonary dose-response to inhaled multi-walled carbon nanotubes. *Nanotoxicology*. 2012
28. Leavens TL, Parkinson CU, James RA, House D, Elswick B, Dorman DC. Respiration in sprague-dawley rats during pregnancy. *Inhal.Toxicol*. 2006; 18:305–12. [PubMed: 22397324]
29. LeBlanc AJ, Moseley AM, Chen BT, Frazer D, Castranova V, Nurkiewicz TR. Nanoparticle inhalation impairs coronary microvascular reactivity via a local reactive oxygen species-dependent mechanism. *Cardiovasc.Toxicol*. 2010; 10:27–36. [PubMed: 20033351]
30. Gokina NI, Mandala M, Osol G. Induction of localized differences in rat uterine radial artery behavior and structure during gestation. *Am.J.Obstet.Gynecol*. 2003; 189:1489–93. [PubMed: 14634590]
31. Moll W, Kunzel W. The blood pressure in arteries entering the placenta of guinea pigs, rats, rabbits, and sheep. *Pflugers Arch*. 1973; 338:125–31. [PubMed: 4734441]
32. Chilian WM, Eastham CL, Marcus ML. Microvascular distribution of coronary vascular resistance in beating left ventricle. *Am.J.Physiol*. 1986; 251:H779–H788. [PubMed: 3766755]
33. Rand RP, Burton AC, Ing T. The tail of the rate, in temperature regulation and acclimatization. *Can.J.Physiol Pharmacol*. 1965; 43:257–67. [PubMed: 14329334]
34. Aukland K, Wiig H. Hemodynamics and interstitial fluid pressure in the rat tail. *Am.J.Physiol*. 1984; 247:H80–H87. [PubMed: 6742216]
35. Osol G, Mandala M. Maternal uterine vascular remodeling during pregnancy. *Physiology*. (Bethesda.). 2009; 24:58–71. [PubMed: 19196652]
36. Thompson LP, Weiner CP. Pregnancy enhances G protein activation and nitric oxide release from uterine arteries. *Am.J.Physiol Heart Circ.Physiol*. 2001; 280:H2069–H2075. [PubMed: 11299208]
37. Nelson SH, Steinsland OS, Suresh MS, Lee NM. Pregnancy augments nitric oxide-dependent dilator response to acetylcholine in the human uterine artery. *Hum.Reprod*. 1998; 13:1361–67. [PubMed: 9647573]
38. Nelson SH, Steinsland OS, Wang Y, Yallampalli C, Dong YL, Sanchez JM. Increased nitric oxide synthase activity and expression in the human uterine artery during pregnancy. *Circ.Res*. 2000; 87:406–11. [PubMed: 10969039]
39. Wu G, Bazer FW, Cudd TA, Meininger CJ, Spencer TE. Maternal nutrition and fetal development. *J.Nutr*. 2004; 134:2169–72. [PubMed: 15333699]
40. Veerareddy S, Campbell ME, Williams SJ, Baker PN, Davidge ST. Myogenic reactivity is enhanced in rat radial uterine arteries in a model of maternal undernutrition. *Am.J.Obstet.Gynecol*. 2004; 191:334–39. [PubMed: 15295388]
41. Kuo L, Davis MJ, Chilian WM. Longitudinal gradients for endothelium-dependent and -independent vascular responses in the coronary microcirculation. *Circulation*. 1995; 92:518–25. [PubMed: 7543382]

42. Stapleton PA, Goodwill AG, James ME, Brock RW, Frisbee JC. Hypercholesterolemia and microvascular dysfunction: interventional strategies. *J.Inflamm.(Lond)*. 2010; 7:54. [PubMed: 21087503]

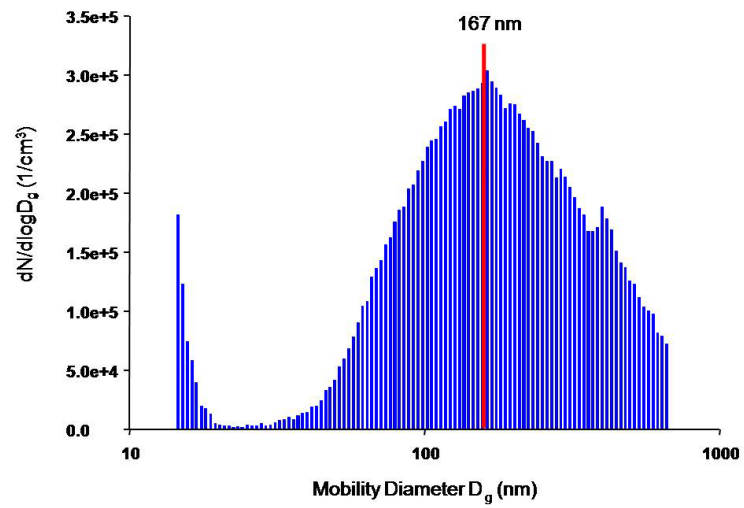
CONDENSATION

The purpose was to evaluate fetal and maternal microvascular consequences of maternal engineered nanomaterial exposure, providing evidence supporting the Barker Hypothesis from a microvascular perspective.

A



B



C

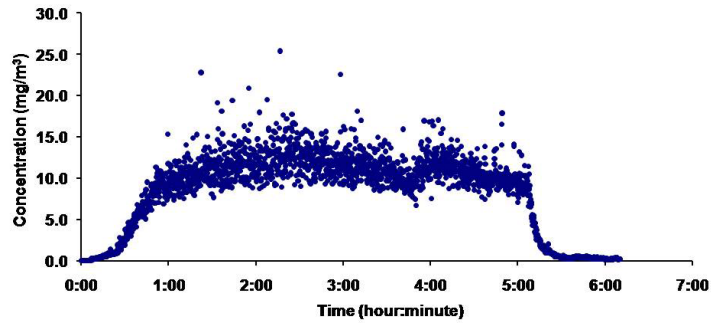
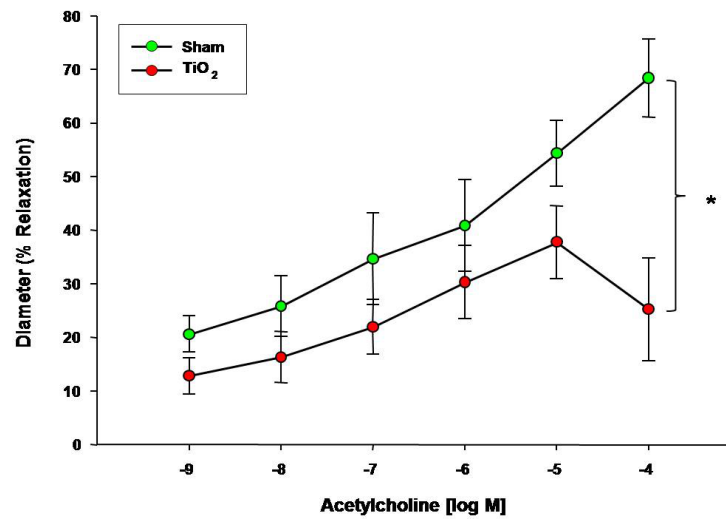


Figure 1. ENM aerosol generation and characterization. Aerosol size distribution and characterization is determined and confirmed using two methods: A) ELPI, which characterizes the mass-based aerodynamic diameter, with a mean of $149 \text{ nm} \pm 3.9$, and B) SMPS, which describes the particle geometric size distribution, with a median of 167 nm . C) A representative image of the daily concentration distribution over the 5-hour exposure, portraying a maintained plateau at $11.2 \text{ mg/m}^3 \pm 0.05$ for the exposure on Jan 23, 2012.

A



B

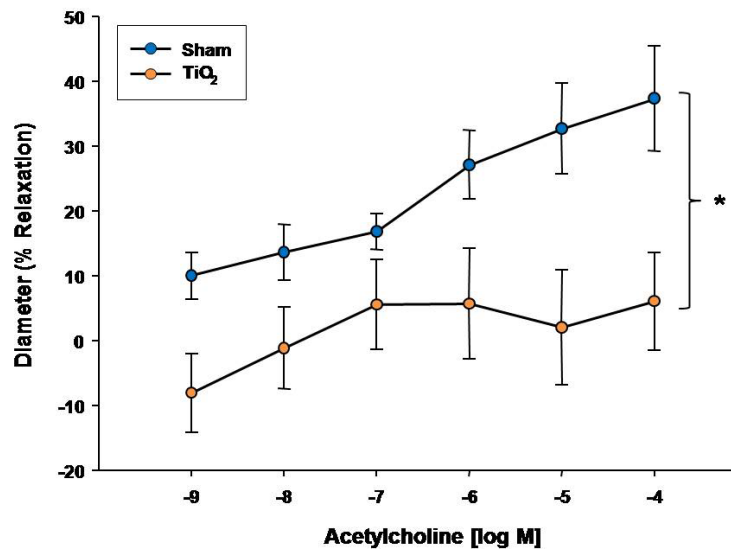
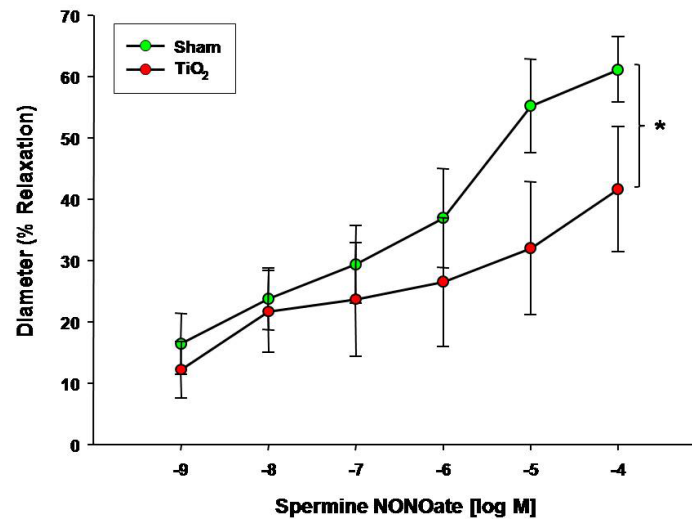


Figure 2. Acetylcholine dose response curve for A) uterine arterioles (n=9-16 vessels). Values are mean \pm S.E. * P < 0.05 sham vs. exposed repeated measures ANOVA. B) fetal tail arteries (n=7-11 vessels) after maternal engineered nanomaterial exposure. * P < 0.05 sham regression line vs. exposed regression line. ENM exposure during pregnancy impairs endothelium-dependent dilation of the uterus and fetus.

A



B

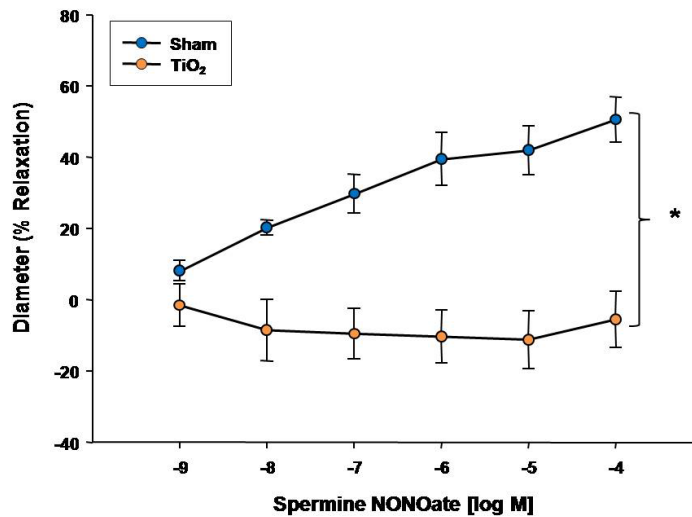
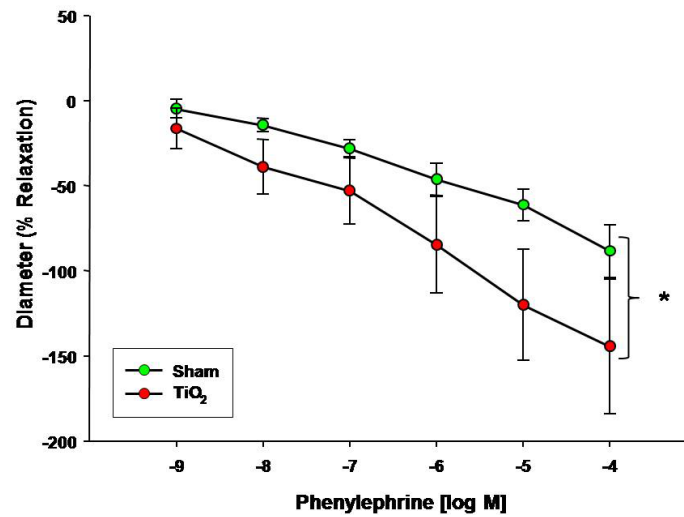


Figure 3. Spermine-NONOate dose response curve for A) uterine arterioles (n=9-16 vessels) B) fetal tail arteries (n=7-12 vessels) after maternal engineered nanomaterial exposure. Values are mean \pm S.E. * P < 0.05 sham regression line vs. exposed regression line. Maternal ENM inhalation impairs maternal and fetal microvascular reactivity to smooth muscle NO signaling.

A



B

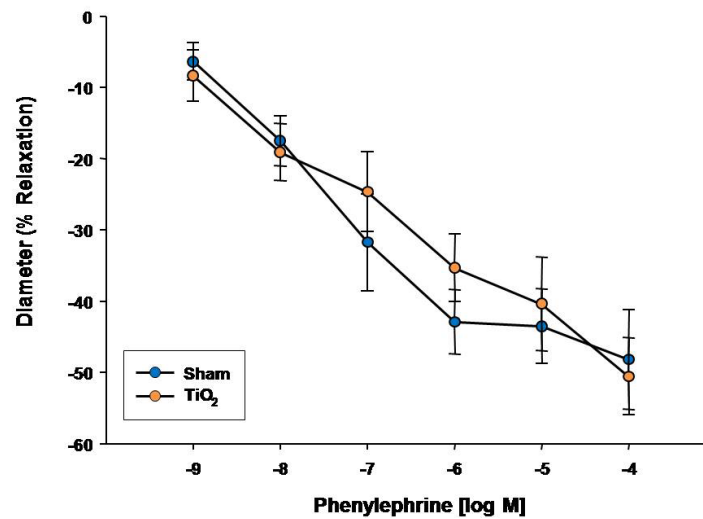
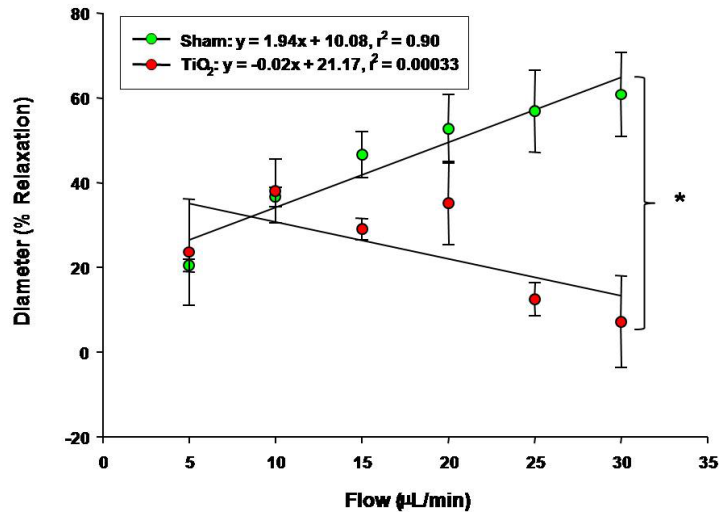
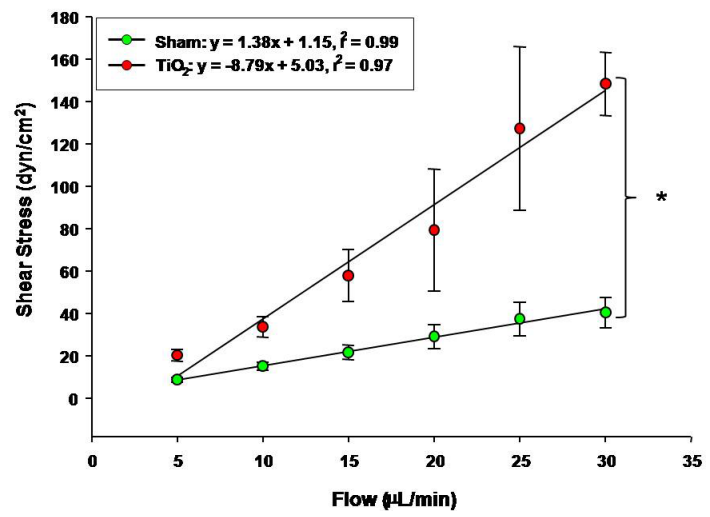


Figure 4. Phenylephrine dose response curve for A) uterine arterioles (n=8-16 vessels) B) fetal tail arteries (n=6-10 vessels) after maternal engineered nanomaterial exposure. Values are mean \pm S.E. * P < 0.05 sham regression line vs. exposed regression line. α -Adrenergic responsiveness was enhanced in uterine vessels, but unchanged in fetal arteries after maternal ENM inhalation.

A



B



C

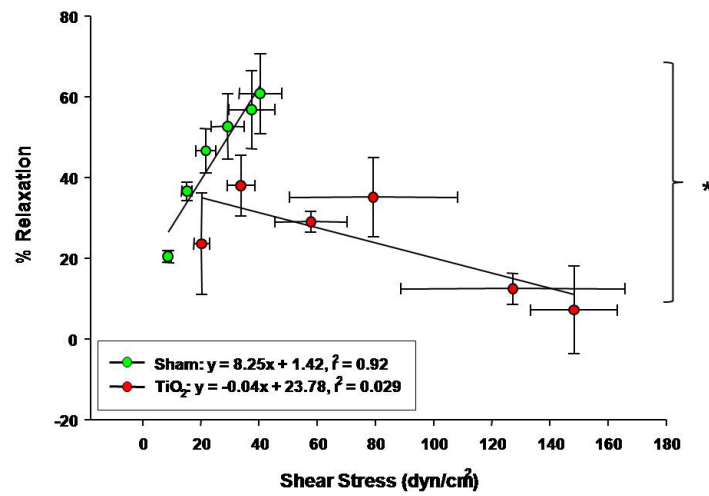
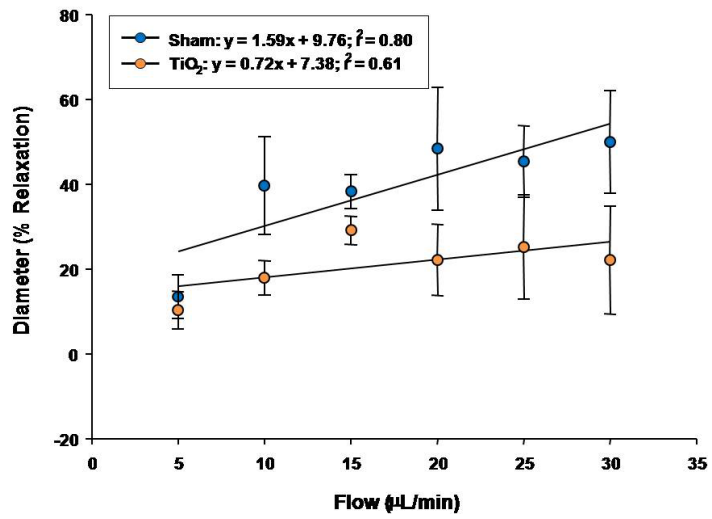


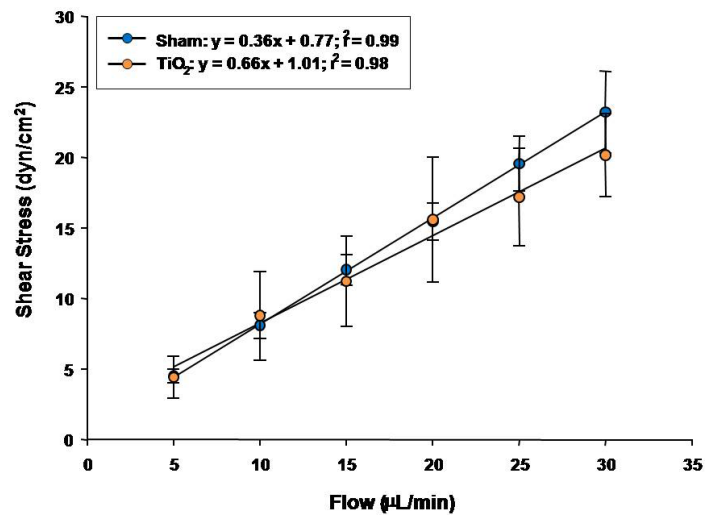
Figure 5.

Uterine arteriolar responsiveness to flow and shear stress after maternal engineered nanomaterial exposure. A) increased intraluminal flow (5-30 $\mu\text{L}/\text{min}$) (4-7 vessels). B) shear stress as a function of flow. C) increased relaxation as a function of increased shear. Values are mean \pm S.E. * $P < 0.05$ sham regression line vs. exposed regression line. Uterine responsiveness to alterations in flow and shear stress is impaired.

A



B



C

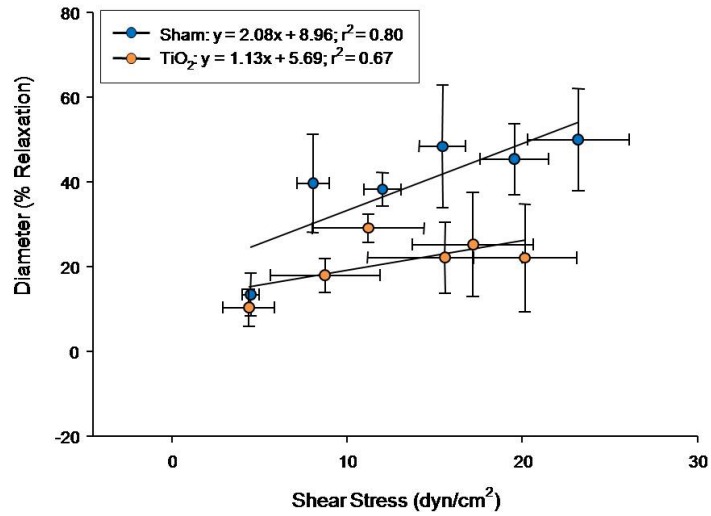


Figure 6. Fetal tail artery responsiveness to flow and shear stress after maternal engineered nanomaterial exposure. A) increased intraluminal flow (5-30 μ L/min) (3-7 vessels). B) shear stress as a function of flow. C) increased relaxation as a function of increased shear.

TABLE 1

Engineered Nanomaterial Exposure and Litter Health

Litter and Exposure characteristics and litter health of pregnant rats exposed to engineered nanomaterial via inhalation.

Treatment	n	Days of Exposure	Aerosol Concentration × Time ((mg/m ³) × hr)	Calculated Total Exposure (μg)	Calculated Total Deposition (μg)	Average Litter Size (number of pups)	Average Litter Weight (g)	Average Weight Per Pup (g)
<i>Sham</i>	6	0	0	0	0	13.25 ± 1.03	42.01 ± 11.86	3.73 ± 0.15
<i>Exposed (total)</i>	10	8.2 ± 0.85	11.31 ± 0.39	380 ± 60	121 ± 19	10.75 ± 1.64	48.01 ± 8.77	4.3 ± 0.49
<i>Exposed (< 7 days)</i>	6	6.33 ± 0.33	10.53 ± 0.37	257 ± 18	82 ± 6	12.16 ± 1.19	58.53 ± 6.49	4.89 ± 0.41
<i>Exposed (> 7 days)</i>	4	11 ± 0.91	12.34 ± 0.19	556 ± 90	178 ± 29	6.5 ± 3.89	16.45 ± 9.86	2.51 ± 0.01

Values are means ± SE.

* P 0.05 sham vs. exposed.

^ P 0.05 exposures greater than 7 days verses exposures 7 days or less.

TABLE 2A

Uterine Microvascular Characteristics

Animal and microvascular characteristics. A) Maternal uterine arteriole.

Treatment	N	Age: Weeks or Gestational Day	Body Weight (g)	Active Diameter (μm)	Passive Diameter (μm)	Vessel Tone
<i>Uterine Sham</i>	9	16.2 w \pm 1.10	403 \pm 17.8	85.89 \pm 6.61	112.33 \pm 6.20	26.91 \pm 2.63
<i>Uterine Exposed</i>	16	14.1 w \pm 0.58	355 \pm 26	66.75 \pm 3.20 [*]	103.06 \pm 4.74	35.47 \pm 2.12 [*]

Values are means \pm SE.

^{*} P 0.05 sham vs. exposed.

TABLE 2B

Fetal Microvascular Characteristics

Animal and microvascular characteristics. B) Fetal tail artery.

Treatment	N	Age: Weeks or Gestational Day	Weight (g)	Active Diameter (μm)	Passive Diameter (μm)	Vessel Tone
<i>Fetal Sham</i>	7	20 d	3.54 \pm 0.17	93.28 \pm 3.87	126.57 \pm 5.92	26.94 \pm 2.49
<i>Fetal Exposed</i>	11	20 d	4.95* \pm 0.33	106.36 \pm 7.56	137.50 \pm 6.45	25.75 \pm 2.75

Values are means \pm SE.

* P 0.05 sham vs. exposed.